J. Geophys. Res., 105, 18495-18503, 2000

Investigation of the conjugacy between auroral breakup and energetic electron injection

L. L. Lazutin,[1,2] L. P. Borovkov,[2] T. V. Kozelova,[2] I. A. Kornilov,[2] V. R. Tagirov,[2] A. Korth,[3] J. Stadsnes,[4] and S. Ullaland[4,5]

Abstract. Auroral TV observations at Loparskaya, Kola Peninsula, and CRRES energetic electron and proton measurements during a moderate isolated substorm at 2000-2100 UT on February 13, 1991, are compared. The CRRES was at the apogee of orbit 494 in the outer radiation belt near the magnetic equator. CRRES footprint projection estimated by using a Tsyganenko magnetic field model was situated at the same latitudes several degrees eastward of active aurora during the substorm breakup or the intensification. The intensification consists of several activations of 1- min duration, and this fine spatial and temporal structure is important for the conjugacy investigations. It is shown that injected energetic electrons have been accelerated at the same time as one of the auroral activations at the same latitude and approximately the same azimuthal extended region. The lack of enhanced electrons during other activations suggests that the acceleration region has a sharp equatorial boundary.

1. Introduction

Auroral substorm morphology is well known: the active phase consists of several discrete intensifications with their own Pi 2 bursts and other onset signatures [*Rostoker et al*, 1980] with or without poleward expansion of the activity. Each intensification consists of several 15 to 90-s activations, which are regarded as an elementary substorm instability. During several minutes of the substorm onset, fast changes of the magnetic field configuration, hot plasma distribution, and other activity signatures in nearly all parts of the magnetosphere occur nearly simultaneously with auroral breakup. This creates a high degree of uncertainity as to which region, either the inner magnetosphere or the plasma sheet boundary layer of the magnetotail, is connected by the magnetic field lines to the active aurora. This will determine which substorm model is more realistic. Therefore the geometry of the magnetospheric substorm and especially the conjugacy of the auroral breakup and associated onset instability in the magnetosphere are the key problems of substorm physics.

In the inner magetosphere at geostationary distances the most powerful events related to auroral substorm activity are sharp energetic particle increases (traditionally called "injections"). Investigation of the injections with energy dispersion gives rise to a suggestion that the particle drift can be described by the injection boundary model [*McIlwain*, 1974; *Mauk and McIlwain,* 1974]. Injections without dispersion indicate particle acceleration in the close vicinity of the satellite and allow the study of spatial structure of the acceleration region [*Arnoldy and Moore*, 1983; *Arnoldy,* 1986; *Lopez et al.,* 1988].

The first coordinated ionosphere-magnetosphere study, based on ATS 5 geostationary satellite measuremen ts [*Akasofu et al.,* 1974; *Mende and Shelley*, 1976], shows that injections are correlated with auroral activity. A study based on magnetic field and particle measurements on board GEOS 2 and aurora in the conjugate region was done by *Kozelova et al.,* [1986]. Both proton and electron increases have been observed simultaneously when the satellite was at the meridian of activation.

Nakamura et al., [1991] studied the spatial structure of substorm intensifications using multipoint aurora observations and particle measurements by two satellites at 6.6 R_E. They found that the active region is restricted in longitude (28 $^\circ$ at the beginning and 40 $^\circ$ at the end of intensification) and that dispersionless electron injections are correlated with N-S aurora, which is the active part of the auroral bulge.

Several examples of coincidence of the active aurora with energetic particle injections at the geostationary region obviously are not reassuring enough because there are numerous publications linking active aurora with more distant regions, such as the magnetotail or the LLBL. Therefore any new data on the geometry of the disturbed magnetosphere are important.

We present here a case study of a moderate isolated magnetospheric substorm at 2000-2100 UT on February 13, 1991. This study is based on aurora observations by the TV camera at Loparskaya Observatory and the energetic particles spectrometer EPAS on board the CRRES satellite, which registered an energetic particle increase associated with this substorm.

The footprint of the CRRES was near the TV camera field of view. We will use this rare occasion of simultaneous observations for a detailed investigation of the fine three-dimensional structure of the disturbances. It is important that both ground-based and satellite data might be inspected with an accuracy of 1 s and better, which allows us to distinguish separate activations in auroral display and particle dynamics and avoid the danger of linking or confusing different events of the activation scale as the same ones.

2. Data Analysis

2.1. Regional Context

Figure 1 presents the map of Kola Peninsula with a field of view of the Loparskaya auroral TV camera (45 ° and 85° zenith angles) and positions of the CRRES footprint during the event.

We calculated the CRRES footprint by using the Tsyganenko 1989 (T-89) and 1996 (T-96) magnetic field models [*Tsyganenko*, 1989, 1996]. Option 3 of T-89, which corresponds to the actual *Kp* index equal to 2, gave footprint coordinates 68.25 °N and 37.55 °E at 2035 UT, which is 4 ° eastward of Loparskaya. The size of the footprint symbols (diamonds) corresponds to options 2 and 4. Similar latitudes (66.8 ° -68.9°N) have been obtained by using the T-96 model, while longitudes estimated by T-96 (38 ° -39° E) are on 1°-1.5° eastward in comparision with T-89.

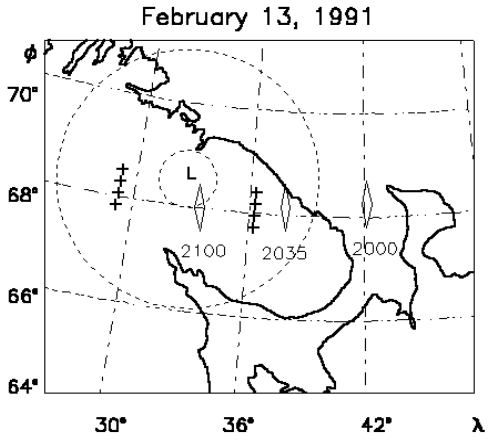

Figure 1. Map of Kola Peninsula with CRRES footprints (center of "diamonds" computed by Tsyganenko 1989, option 3, and the size using options 2 and 4). Large circle centered at L (Loparskaya) shows TV all-sky camera field of view; small circle corresponds to half-radius circle of the TV pictures, or half width of the keogram shown by Plate 1. Crosses indicate the position of the approximated azimuthal boundaries of the particle source region.

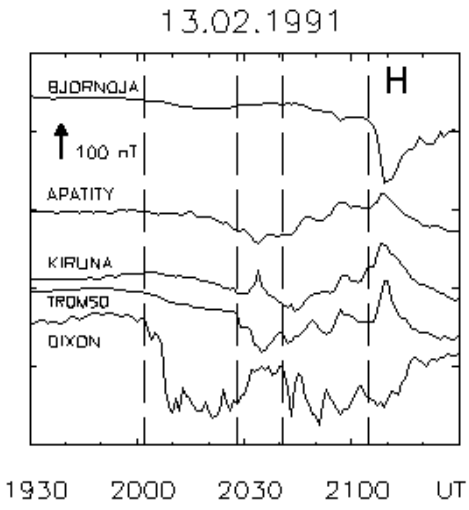

Figure 2. *H* component of the magnetometer records of several auroral zone stations. Dashed lines show the beginning of the four substorms or intensifications.

2.2. Magnetic Variations

Figure 2 presents 2 hours of the *H* component of several auroral zone magnetograms. The magnetospheric substorm was relatively weak (-300 nT) and fairly complicated. It consisted of several intensifications, separated in time and space with their individual auroral breakups and negative magnetic *H* bays. Possibly it was not a single substorm but three or four overlapping substorms.

In the magnetometer records, four main decreases of the *H* component are observed. The first bay was registered from 2000 UT to 2030 UT at the meridian of Dixon (73.6 °N, 80.6° E). The second one was centered in Scandinavia. A magnetometer in Apatity (67.5°N, 33.3°E) shows that a gradual negative bay started at 2015 UT with a minimum of *H* component at 2033 UT, whereas two sharp drops have been registered in Tromso (69.7°N, 19.0°E) at 2028 and 2032 UT. The third intensification began at 2040 UT in a wide sector, from Dixon to Kiruna (67.8°N, 20.4°E), and the last one which started at 2105 UT was shifted poleward, with its minimum *H* component at Bjornoya (74.5°N, 19.2°E). It is the second substorm which will attract our attention, because additional auroral TV observations were available for that time.

2.3. CRRES Observations

CRRES is in a geostationary transfer orbit with 6.3 R_E apogee. During the intensification discussed above it was in the midnight sector, near the magnetic equator and at apogee. We have used data from the magnetometer [*Singer et al*., 1992] and the energetic particle spectrometer EPAS [*Korth et al.*, 1992], which has 14 electron and 12 proton differential energy channels and covers the energy range from 21.5 to 285 keV and from 37 to 3200 keV, respectively.

According to the particle pitch angle distrib utions, CRRES was in the outer radiation belt, well inside the trapping boundary. It is a typical position of the satellite during injection events [*Reeves et. al.,* 1996; *Lazutin and Korth*, 1998].

Figure 3 presents half-minute-averaged electron and proto n fluxes for several differential energy channels and the total magnetic field magnitude. There are two apparent intensity increase events in this picture, one in the proton flux associated with first intensification and another, in electron intensity, coinciding with the second substorm. The absence of

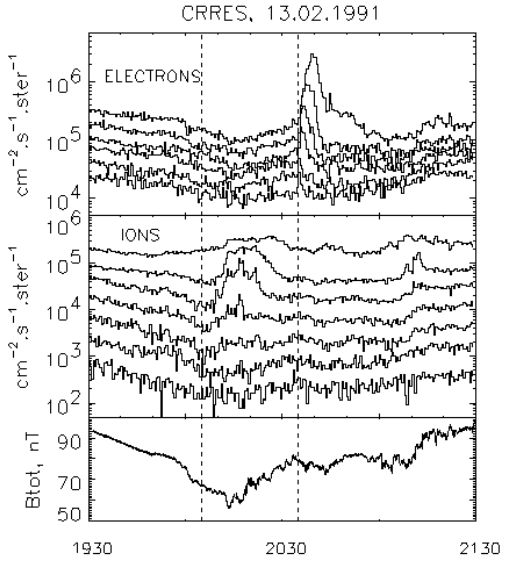

Figure 3. Half-minute-averaged intensities of six electron differential channels (21.5-112 keV) and seven proton channels (37-254 keV) measured on CRRES orbit 494. (bottom) Total magnetic field, $\Delta T = 2$ s.

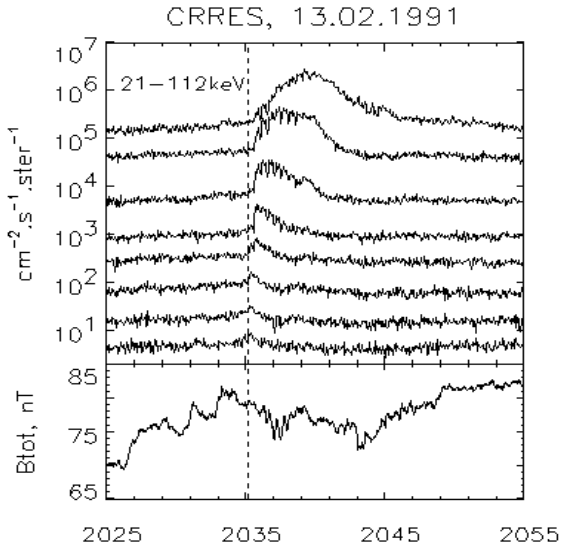

Figure 4. Energetic electron injection temporal structure with 2-s resolution, channels 1 to 8 (energy limits in keV: 21.5-31.5-40-49.5-59-69-81-94.5-112). (bottom} Total magnetic field magnitude.

the electron enhancement and energy dispersion of the proton increase indicate, that the satellite was located westward of the acceleration region during the first event (cf. the Dixon magnetic bay in Figure 2). Injected electrons drift in the opposite direction so that CRRES did not see them, but other consequences of the breakup are present: gradual increase of the magnetic field magnitude and of the background particle intensity level are both signatures of the magnetic field dipolarization. Likewise during the second event, absence of the proton increase and small, but distinctive electron energy dispersion suggest, that the substorm active region was located slightly westward of the satellite in accordance with magnetometer data.

The spin period of CRRES is 30 s, which determines the lower limit of the temporal resolution of the entire particle distribution function. Better resolution can be achieved by using intensity information without complete knowledge of the pitch angle distribution. Figure 4 presents an expanded view of the electron increases in different energy channels integrated over 2 s, notwithstanding the pitch angle. In this figure a time delay of the intensity maximum in different energy channels is observed. This could be used to calculate the drift path of the enhanced electrons from the distant border of the acceleration region. For the calculation of the gradient drift velocity the magnitude of the magnetic field at the magnetic equator and radial gradient are needed, which we found for 2035 UT using option 3 of the Tsyganenko 1989 model.

Figure 5 shows the result of the backtracking of particle drift trajectories calculated for several energy channels based on experimental time delay values. We chose as *To* = 2035:10 UT the moment of intensity maximum in the 100-keV channel and as zero longitude the position of the CRRES. On the positive part of the timescale additional delays of lower- energy channels are marked as a final time of the electron drift. At the negative part of the timescale all five velocity lines intersect at one point equal to –55 s. Therefore it can be concluded that all electrons which received maximum acceleration rate started at the distance of 7.2° from CRRES 55 s before *To*. It is necessary to mention that the calculated drift time is independent of the choice of the magnetic field model because only experimental delay values and the ratio of the drift velocities are important.

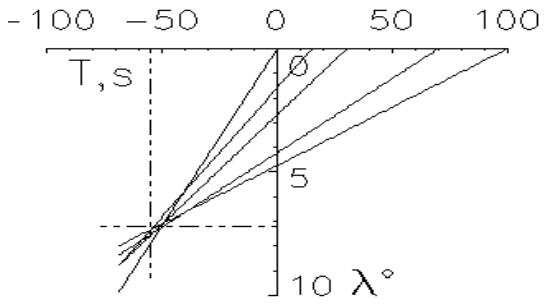

Figure 5. Calculated drift trajectories of the electrons of channels 2, 3, 5, 6 and 8. Latitudinal distances is in degrees; time in seconds. T_o = 2035:10 UT is the moment of intensity maximum in 100-keV channel, and $\lambda° = 0$ is the position of CRRES.

It is possible to correct t he calculated duration by taking into account that electrons registered by CRRES detectors started to drift with a smaller energy and therefore with a smaller drift velocity. As will be shown below, the energy gain might be estimated as 30 keV, which means that the initial drift velocity was 0.7 of the final velocity for 100-keV electrons. Assuming a linear change of drift velocity, we calculate a 65 s drift duration instead of 55 s. That means that the associated activation started at about 2034:05 UT.

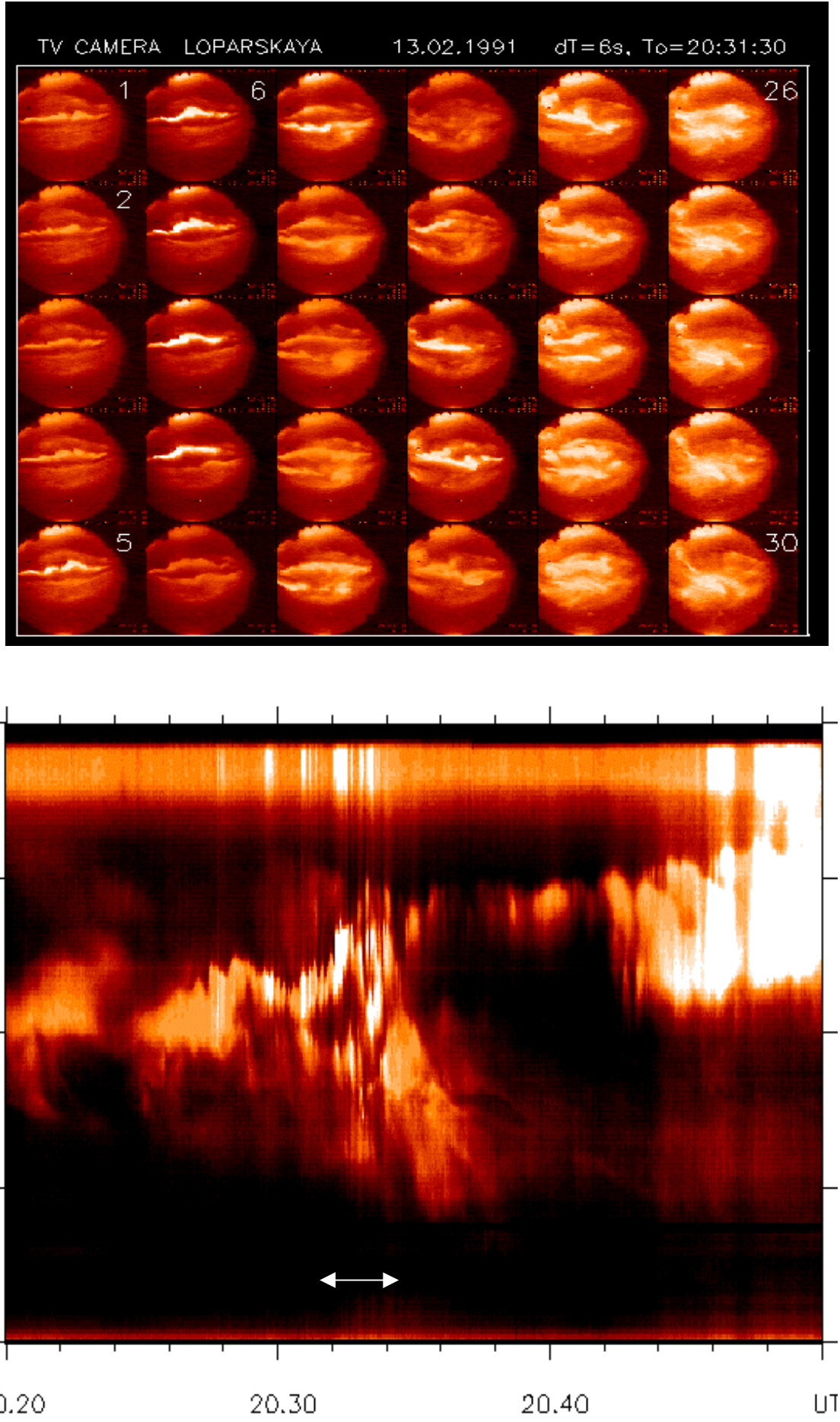

Plate 1. (top) TV all-sky snapshots from Loparskaya Observatory with 6-s resolution during second substorm. South is on the bottom, and east at the left side of the frames. Time is directed from top to bottom and from left to right. (bottom) Keogram of the aurora brightness at the central Loparskaya magnetic meridian. Note nonlinear latitude scale. White bar indicates time interval of the TV frame panel.

2.4. Aurora

Loparskaya Observatory of the Polar Geophysical Institute is situated at the northern part of the Kola Peninsula (68.62°N, 33.3°E). Plate 1 presents in pseudocolor the keogram showing temporal variation of the N-S cross-section of the auroral luminosity created from the TV records for a 30-min interval and the sequence of TV frames with $dT = 6$ s for shorter time periods around the breakup.

The TV camera was put into operation at 2016 UT, when the aurora, related to the first Dixon substo rm, appeared over Loparskaya. It was a widely diffused arc system near the zenith, which became a cradle for the second Kola intensification. Before the breakup (2032 UT), three brightenings of the arc were registered; the last two can be found on the keogram at 2020 and 2025 UT. It is a typical prebreakup phenomenon. The diffused area close to the northern horizon was not active, and the shape and brightness remained the same throughout the interval under consideration.

The breakup was short; it started at 2031:55 and ended at 2038 UT. As can be seen from Plate 1, it was divided into three activations, with a duration of about 1 min. It was possible to observe a restricted poleward expansion in every activation, but the latitudinal position of the second and third activation moves steplike to the south.

The most intense (first) activation started at 2031:55 UT, and the second one started at 2033:20 UT. Both activations occur before the calculated electron injection time. Only the third activation, which began at 2033:45 UT and which was less intense than the first two, approximately coincides with the injection time.

Using the keogram data file, several simulations were created of the photometric records with photometers looking to the zenith at different positions along the Loparskaya magnetic meridian. Figure 6 presents the resulting variations of the aurora brightness. The levels of the records are shifted to separate three groups of the photometers at different latitudes. The vertical line indicates the starting time of the injection, as estimated above from electron energy dispersion. In the bottom panel, magnetic Pi 2 pulsations are presented, registered by the Lovozero Observatory which is situated 150 km to the south and 70 km to the east from Loparskaya. It is interesting to note that the most intense first activation has a small Pi 2 amplitude; for such localized events the relative distance between the footprint of the source region and the magnetometer position might be important. Likewise, the magnetic variations registered by CRRES in general reflect the dipolarization process from 2010 to 2035 UT, but the fine structures do not coincide with auroral activations.

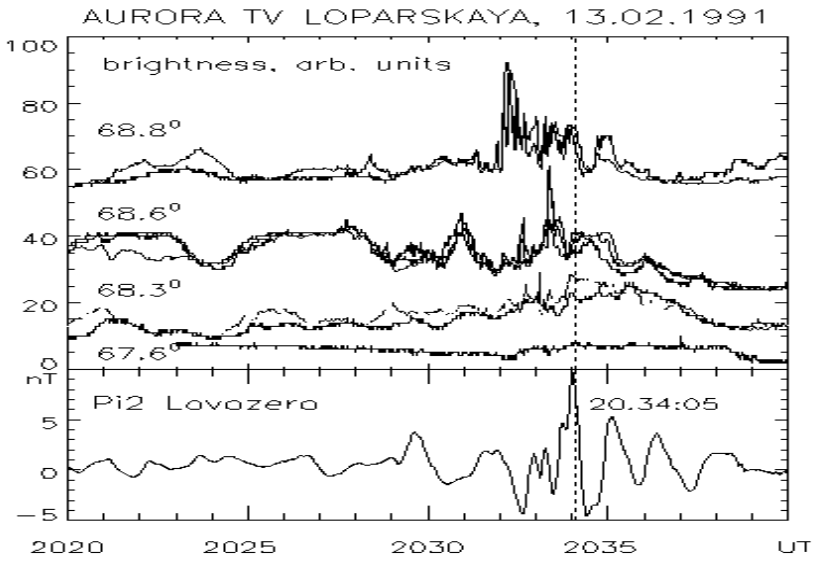

Figure 6. Synthetic zenith photometer records at four sections of the Loparskaya meridian during three auroral activations. Two or three neighboring points were used to show data deviation. Dashed line, calculated starting time of the electron acceleration. (bottom) Magnetic Pi 2 pulsations (*H* component) registered in Lovozero

2.5. Comparison of the Observations

It is difficult to assume that activations 1 and 2 did not generate energetic electrons. Most probable, the electron clouds from the first two activations pass outside of the CRRES orbit on their magnetic drift. If that is true, then the energetic electron acceleration region must have sharp equatorial boundaries similar to and at the same position as the auroral activations. And only the third auroral activation was situated conveniently for the registration by CRRES detectors.

The dashed line in Figure 6, which corresponds to the calc ulated time of the beginning of the energetic electron acceleration, is delayed by 10 s in comparision with the beginning of activation. It can be ascribed to the uncertainty of the delay timing, but careful inspection of the TV record shows that the third activation, which begins at 2033:45 UT , shifts

further southward at 2034:00-2034:20 UT. We cannot find an additional intensity maximum at 68.2 ^{0} in the keogram, because the corresponding aurora activation occurs westward of the central meridian. Therefore the beginning of the CRRES energetic electron injection may exactly coincide with the third activation if we take into account the 10- to 15- s delay of southward activity propagation.

We found above the western boundary of the acceleration region. Addi tional information can be extracted from the electron intensity time profiles (Figure 4) about the CRRES footprint position with respect to the eastern edge of the acceleration region. At the beginning of the increase, before the maximum, we observe the arrival of electrons from the nearest part of the acceleration region. The increase of intensity started in electron energy channels 5 and 6 at 2035 UT. Using the results of the calculation of the magnetic drift shown in Figure 5, the longitudinal distances from the CRRES can be estimated as 2 °-3°. It is not exactly the distance between CRRES and the nearest border of acceleration region; it has to be smaller than 2 °, because particles must spend a certain time in the acceleration region to gain energy. It is possible to find a more accurate value, because we know that the satellite is moving westward toward the acceleration region (0.3 deg/min) and must soon enter it. A sharp increase of the electron intensity with pancake pitch-angle distribution was registered in channels 2 to 4 at 2035:40 UT . It can be interpreted as an encounter of the satellite with the region of enhanced electron population.

Therefore at 2035 UT, the CRRES footprint was 0.3 ^{0} eastward from the nearest edge of the energetic particle acceleration region and 7.5 ^{0} from the distant one, the total longitudinal dimension and position approximately the same as those for the third auroral activation. Therefore all results of data analysis and comparison are in agreement with an assumption that the western edge, the eastern edge, and the equatorial boundary of the active aurora and energetic electron acceleration region are located close to each other.

The eastern border of the aurora was situated at the moment approximately at 36.5 ^{0} E $\pm$ 0.5^0. (The position of the aurora near the horizon, at the edge of the TV frame and indistinct boundary, does not allow better resolution.) The latitude of the CRRES footprint predicted by the T-89 model at the moment of encounter with the acceleration region was equal to 37.5^0 . The difference of 1 ° is insignificant, taking into account the statistical origin of the Tsyganenko model; therefore this comparison confirms the assumption that the active aurora and the energetic electron acceleration region are identical.

Figure 7 presents energy spectra of the CRRES electrons for the five moments indicated in the insert at the top right corner. Comparing the spectrum at the maximum intensity for a certain energy with the initial spectrum, we can estimate the magnitude of the electric field applied to the electrons. Intensity of the 90-keV electrons at the moment B is equal to the intensity of 60-keV electrons in the undisturbed spectrum A. Intensity of 60-keV electrons at the moment C corresponds to 30 keV of spectrum A. Therefore we can estimate that the total electric potential was of the order of 30 kV.

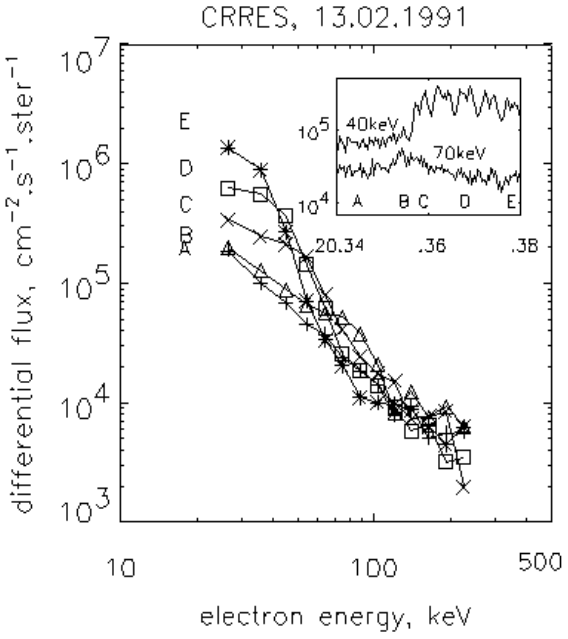

Figure 7. Electron energy spectra at several time intervals with consecutive arrival of electrons with lower energies.

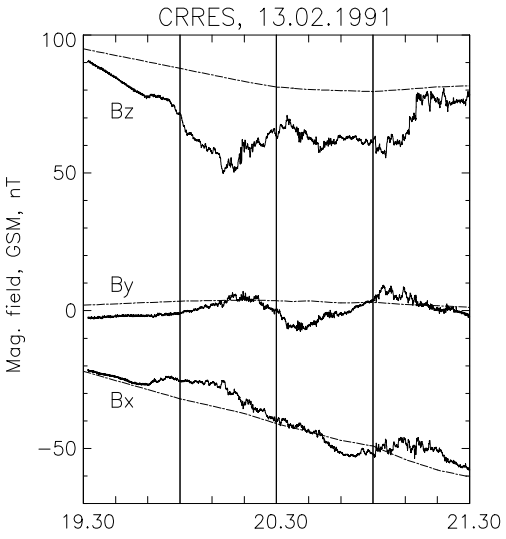

Figure 8. Three components (GSM) of the magnetic field measured by the CRRES magnetometer. Dashed lines present the same components calculated by using option 3 of the Tsyganenko 1989 model.present the same components calculated by using option 3 of the Tsyganenko 1989 model.

3. Discussion

Two events have been registered: auroral breakup by a ground-based TV camera and energetic electron increase in the magnetosphere. Let us start with the identification or classification of these two events and proceed with the main experimental results of the comparison.

1. The increase of the electron intensity, as observed in our study, is a typical phenomenon well known as an injection event. When CRRES on other orbits was situated closer to the center of the acceleration region, dispersionless injections were observed in both electrons and ions, accompanied by magnetic field dipolarization [*Rasinkangas et al*., 1994, 1996]. Usually the fine temporal structure of the injection event is more complicated; several elementary activations might be recognized by superimposed effects in enhanced electron flux [*Lazutin et al.,* 1998a]. In our case, only one activation is registered with a typical increase for a single- activation duration of the acceleration and the rate of intensity.

2. Auroral intensifications also have activation scale time structure. Inspection of the spatial and temporal fine structure of the energetic electron and auroral activations shows that they are very similar [*Lazutin,* 1999]. In our case, three auroral activations with consequent southward shift have been registered.

3. We have used the Tsyganenko 1989 model for the first step approximation of the magnetic field line projection from the magnetosphere to the ionosphere. Direct comparison of the measured, in our case, and calculated magnetic field during 2 hours of the CRRES flight is presented in Figure 8. While B_x and B_y show good agreement, the measured Z component value remains lower than that predicted until the last dipolarization step at 2115 UT. Therefore one can conclude that if the equatorial part of the magnetic field line predicted by the T-89 model differs from the measurements, it must be more taillike. It is necessary to mention that the Tsyganenko model, as many others , has certain restrictions. *Reeves et al.,* [1996] show that the model footprint is in agreement with the measured ones with only a 32% probability within the error bar of $\pm 1^\circ$ shown in Figure 3 but that our event seems to lie within that 32%.

4. For the investigation of the conjunction it is important to have good coincidence in time for the effects that are compared. Indeed, during several minutes of breakup , dynamical processes have been registered in almost all magnetospheric main regions: radiation belts or inner magnetosphere, magnetotail, boundary layers, and in a cusp region. Therefore coincidence or delay of the processes, separated in space with an accuracy of 1-2 min does not provide motive for the reasonable conclusions.

As we pointed out earlier, substorm intensifications are divided into several activations of 15- to 100-s duration. If it is correct that activations are the elementary structures of the substorms [*Rasinkangas et al.,* 1996*; Lazutin*, 1999; *Lazutin et al.,* 1998a], then any identification of the events widely separated in space makes sense only if the temporal link is less than 1 min. Otherwise, two different activations might be considered as the same event. Using Plate 1, one can create poleward or equatorward propagation of the activity by choosing the position of two satellites on different latitudes if one ignores that they register different activations.

In our case study we escaped this difficulty, because from the TV data we know about three auroral activations and were able to identify a single one. We can explain the absence of the energetic electron during the first two activations and coincidence of the energetic electron injection during the third activation only by assuming a unique combination of the satellite footprint position and particle source shape.

5. Good coincidence of the field line tubes where energetic electrons are accelerated with that of the electr ons responsible for the active aurora is the most important point of this study. We cannot claim that these areas are totally identical because we have no information on the position and the shape of the poleward boundary, but longitudinal position and extension are similar and both areas have a sharp southward (earthward) boundary.

6. This coincidence is not an anticipated result, because low-energy (1-10 keV) auroral particles and energetic ones (20-500 keV) are supposed to be accelerated by different mechanisms: the first ones by a field-aligned electric field and the second ones by an induced electric field.

7. As a result of the comparison it is possible to conclude that acceleration of the energetic electrons is the succession of several short injections located at the restricted areas, rather than a wide injection front [*McIlwain,* 1974]. That in fact is not a new conclusion but has been suspected for a long time, for example, from the multiballoon measurements of auroral X rays [*Bjordal et al*., 1971; *Pytte et al.,* 1976; *Zhulin et al.,* 1976; *Melnikov et al*., 1978; *Kremser et al*., 1982; *Lazutin et al.,* 1998b].

8. Coincidence of their spatial areas does not agree well with the existing model of drift current disruption [*Lui et al.,* 1988, 1992]. This model among possible models of substorm onset still seems to be the most acceptable for an explanation of the results of this case study. But if the magnetic field dipolarization is an effect of localized current disruption with a single field-aligned current loop, then the region where dB is positive and where induced electric fields are generated will not be so restricted, and we will not observe a sharp earthward boundary of the acceleration region. Also, at the satellite position the dipolarization effect would not be so smooth and small. Therefore we need geometry of the instability that will be capable of explaining the restricted areas of both field-aligned and equatorial particle acceleration. Possibly, it is necessary to incorporate the magnetotail current meander model suggested by *Heikkila and Pellinen* [1977] and *Pellinen and Heikkila*, [1978, 1984], applied not to the tail, but to the radiation belt region. According to this model, the induced electric field during activation appears in the restricted meander region with sharp southward and northward boundaries. The formation of the meander can be stimulated by a local decrease or increase of the drift current due to the radial displacement of the drifting particles during magnetic field reconfiguration.

Moreover, it is quite possible that the assumption that the breakup auroral particle and energetic electron injection demands two separate acceleration mechanisms is a mistake. Possibly, the meander model may be combined with a current disruption model with simultaneous particle acceleration over a wide energy range, but of course all of that needs special consideration.

4. Conclusion

Let us summarize the results of data analysis. At the beginning, we observe that the increase of the energetic electrons registered by the CRRES detectors did not exactly coincide in time with any auroral activations near the calculated footprint. But the energy dispersion of the increase and the absence of the simultaneous magnetic field dipolarization suggest that the associated activation where energetic electrons have been accelerated occurs approximately 1 min before and several degrees to the east of the CRRES magnetic field tube. The calculation of source position, geometry, and timing using differential particle drift effects suggests that experimental observations from the ground and in the equatorial plane agreed most favorably with the assumption that the energetic electron acceleration region coincides with the third activation of the auroral breakup. That means that energetic electrons might be accelerated simultaneously and on the same magnetic field line tube as auroral electrons associated with an active aurora. The absence of an increase of the CRRES energetic electrons corresponding to the previous and following auroral activations allows us to find a more precise estimation of the CRRES footprint position and suggests that the regions of the acceleration of the energetic electrons have sharp equatorward boundary, longitudinal position, and extension coinciding with those of associated active auroras.

Among possible models of substorm onset, the model of current disruption in the inner magnetosphere seems to be the most acceptable for an explanation of the results of this case study. However, the geometry of the disruption must be more complicated than a single current wedge and must create multiple localized particle acceleration regions, which is possible if the substorm meander model will be incorporated.

Acknowledgments. The authors are very grateful to I. Okunev and other workers of the PGI ground-based observatories for the data used in this study and to H. Singer for providing CRRES magnetometer data. One of the authors (L.L.L.) wishes to thank his friend, John R. Crenshaw, for his assistance with the English in this paper. John Crenshaw passed away on November 22, 1999 in San Antonio, Texas.

Michel Blanc thanks Roger Arnoldy and another referee for their assistance in evaluating this paper.

References

Akasofu, S.-I., S. DeForest, and C. McIlwain, Auroral displays near the "foot" of the field line of the ATS-5 satellite, *Planet. Space Sci., 22*, 25-30, 1974.

Arnoldy, R. L. Fine structure and pitch angle dependence of synchronous orbit electron injections. *J. Geophys. Res., 91*, 13,411-13,421, 1986.

Arnoldy, R. L., and T. E. Moore, Longitudinal structure of substorm injections at synchronous orbit, *J. Geophys. Res., 88,* 6213-6220, 1983.

Baker, D. N., and T. I. Pulkkinen, The earthward edge of the plasma sheet in magnetospheric substorms, in *Magnetospheric Substorms, Geophys. Monogr. Ser., vol. 64,* edited by J. R. Kan, T. A. Potemra, S. Kokubun, and T. Iijima, pp.147-160, AGU, Washington, D. C., 1991.

Bjordal, J., et al., On the morphology of auroral X-rays events, 1, Dynamics of midnight events, *J. Atmos. Terr. Phys., 33*, 605-620, 1971.

Heikkila, W. J., and R. J. Pellinen, Localized induced electric field within the magnetotail, *J. Geophys. Res., 82*, 1610-1614, 1977.

Hultqvist, B., et al., Simultaneous observation of upward moving field-aligned energetic electrons and ions on auroral zone field lines, *J. Geophys. Res., 93*, 9765-9776, 1988.

Korth, A., G. Kremser, B. Wilken, W. Guttler, S. L. Ullaland, and R. Koga, Electron and proton wide-angle spectrometer (EPAS) on the CRRES spacecraft, *J. Spacecr. Rockets, 29,* 609-614, 1992.

Kozelova T.V., J-P. Treilhou, A. Korth, G. Kremser, L. Lazutin, A. O. Melnikov, A. Pedersen, Ya. A. Sakharov, Substorm active phase study by ground-based and satellite measurements, *Geomagn. Aeron., 26*, 963-969, 1986.

Kremser, G., et al., Coordinated balloon-satellite observations of energetic particles at the onset of the magnetospheric substorm, *J. Geophys. Res., 87*, 4445-4455, 1982.

Lazutin L., Substorm activations: comparison of fine structures. *Adv. Space Res., 23, No. 10,* 1671-1674, 1999.

Lazutin, L., and A. Korth, Distribution of energetic particle "injections" events along the radiation belt slope, *Substorms-4,* edited by S. Kokubun and Y. Kamide, pp. 817-820, Terra, Tokyo, 1998.

Lazutin L. L., R. Rasinkangas, T. V. Kozelova, A. Korth, H. Singer, G. Reeves, W. Riedler, K. Torkar, and B. B. Gvozdevsky, Observations of Substorm Fine Structure, *Ann. Geophys., 16,* 775-786, 1998a.

Lazutin, L., W. Riedler, K. Torkar, and J.P. Treilhou, Magnetospheric substorm studies using scientific balloons, in *Abstracts of 32nd Scientific Assembly of COSPAR, 12-19 July 1998, Nagoja, Japan*, p. 478, COSPAR, Paris, 1998b.

Lopez, R. E., D. N. Baker, A. T. Y. Lui, D. G. Sibeck, R. D. Belian, R. W. McEntire, T. A. Potemra, and S. M. Krimigis, The radial and longitudinal propagation characteristics of substorm injections, *Adv. Space Res., 8,* 91-95, 1988.

Lui, A. T. Y., R. E. Lopez, S. M. Krimigis, R. W. McEntire, L. J. Zanetti, and T .A. Potemra, A case study of magnetotail current sheet disruption and diversion, *Geophys. Res. Lett., 15,* 721-724, 1988.

Lui, A .T. Y., R. E. Lopez, B. J. Anderson, K. Takahashi, L. J. Zanetti, R. W. McEntire, T. A. Potemra, D. M. Klumpar, E. M. Greene, and R. Strangeway, Current disruptions in the near-Earth neutral sheet region, *J. Geophys. Res., 97*, 1461-1480, 1992.

Mauk, B. H., and C. E. McIlwain, Correlation of *Kp* with the substorm-injected plasma boundary, *J. Geophys. Res., 79*, 3193-3196, 1974.

McIlwain, C. E., Substorm injection boundaries, in *Magnetospheric Physics,* edited by B. M. McCormac, pp. 143-154, D. Reidel, Norwell, Mass., 1974.

Melnikov, A. O., et al., X-ray burst structure during a breakup and geomagnetic pulsations of Pi2 type, in *Dynamic processes and the auroral magnetosphere structure (" SAMBO" experiment*) (in Russian), p. 28-42, Acad. of Sci. of the USSR, Apatity, Russia, 1978.

Mende, S. B., and E. G. Shelley, Coordinated ATS-5 electron flux and simultaneous auroral observations, *J. Geophys. Res., 81*, 97-100, 1976.

Nakamura, R., T. Oguti, T. Yamamoto, S. Kokubun, D. N. Baker, and R. D. Belian, Aurora and energetic particle signatures during a substorm with multiple expansions, in *Magnetospheric Substorms, Geophys. Monogr. Ser.,* vol. 64, edited by J. R. Kan, T. A. Potemra, S. Kokubun, and T. Iijima, pp.285-294, AGU, Washington, D. C., 1991.

Pellinen, R. J. and W. J. Heikkila, Energization of charged particles to high energies by an induced substorm electric field within the magnetotail, *J. Geophys. Res., 83*, 1540-1550, 1978.

Pellinen, R. J. and W. J. Heikkila, Inductive electric fields in the magnetotail and their relation to auroral and substorm phenomena, *Space Sci. Rev., 37*, 1-61, 1984.

Pytte, T., H. Trefall, G. Kremser, P. J. Tanskanen, and W. Riedler, On the orphology of high-energy (>30 keV) electron precipitation at the onset of negative magnetic bays, *J. Atmos. Terr. Phys., 38*, 757-773, 1976.

Rasinkangas, R., V. A. Sergeev, G. Kremser, T. Ulich, H. J. Singer, and A. Korth, 0Current disruption signatures at substom onset observed by CRRES, in *Proceedings of the Second International Conference on Substorms* , edited by J. R. Kan, J. Craven, and S.-I. Akasofu, p.595, Geophys. Inst., Fairbanks, Alas., 1994.

Rasinkangas, R., et al., Observations of substorm onset and injection boundary deep in the inner magnetotail, in *Proceedings of the Third International Conference on Substorms (ISC-3), Versailles, France, 12-17 May 1996, Eur. Space Agency Spec. Publ., ESA SP-389,* 573-578, 1996.

Reeves, G. D., L. A. Weiss, M. F. Thomsen, and D. J. McComas, Quantitative experimental verification of the magnetic conjugacy of geosynchronous orbit and the auroral zone, in *Proceedings of the Third International Conference on Substorms (ICS-3), Versailles, France, 12-17 May 1996, Eur. Space Agency Spec. Publ., ESA SP-389*, 187-192, 1996.

Rostoker, G., S.-I. Akasofu, J. Foster, R.A. Greenwald, Y. Kamide, K. Kawasaki, A.T.Y. Lui, and R. L. McPherron, Magnetospheric substorms: Definition and signatures, *J. Geophys. Res., 85*, 1663-1668, 1980.

Singer, H. J., W. P. Sullivan, P. Anderson, F. Mozer, P. Harvey, J. Wygant, and W. McNeil, Fluxgate magnetometer instrument on the CRRES, *J. Spacecr. Rockets*, *29,* 599-601, 1992.

Tsyganenko, N. A., A magnetospheric magnetic field model with a warped tail current sheet, *Planet. Space Sci., 37*, 5-20, 1989.

Tsyganenko, N. A., Effects of the solar wind conditions on the global
magnetospheric configuration as deduced from data-based field models, in *Proceedings of the Third International Conference on Substorms (ISC-3), Versailles, France, 12-17 May 1996, Eur. Space Agency Spec. Publ., ESA SP-389,* 181-185, 1996.

Zhulin, I. A., et al., Soft and hard auroral X-ray bursts in midnight sector measured in SAMBO experiment, in *Magnetic Disturbances and Processes in Auroral Zone* (in Russian), pp. 48-68, Acad. of Sci. of the USSR, Apatity, Russia, 1976.

L. P. Borovkov, I. A. Kornilov, T. V. Kozelova[1], and V. R. Tagirov, Polar Geophysical Institute, Russian Academy of Sciences, Apatity, Murmansk Region, 184200, Russia. (borovkov@pgi.kolasc. net.ru; kornilov@pgi.kolasc.net.ru; kozelova@pgi.kolasc.net.ru; tagi- rov@pgi.kolasc.net.ru)

A. Korth, Max-Planck-Institut fur Aeronomie, D-37191 Katlenburg-Lindau, Germany. (korth@linmpi.mpg.de)

L. L. Lazutin, Space Physics Division, Skobeltsyn Institute of Nuclear Physics, Moscow State University, Vorobjevy Gory 119899, Moscow, Russia. (lazutin@srdlan.npi.msu.su)

J. Stadsnes, Department of Physics, University of Bergen, Allegt. 55, N-5007 Bergen, Norway. (Johan.Stadsnes@fi.uib.no)

(Received April 23, 1998; revised August 22, 1999;
accepted January 31, 2000.)

[1]Now at Skobeltsyn Institute of Nuclear Physics, Moscow State University, Moscow, Russia.
[2]Polar Geophysical Institute, Russian Academy of Sciences, Apatity, Russia.
[3]Max-Planck-Institut fur Aeronomie, Katlenburg-Lindau, Germany.
[4]Department of Physics, University of Bergen, Bergen, Norway.
[5]Deceased October 1998.